A Study of Relationships in Traffic Oscillation Features Based on Field Experiments

Handong Yao, Qianwen Li, Xiaopeng Li*

Department of Civil and Environmental Engineering, University of South Florida, 4202 E Fowler Avenue, ENC 3300, Tampa, FL 33620

Abstract

Despite numerous theoretical models, only limited field experiments have been conducted to investigate traffic oscillation propagation, and the relationships between traffic oscillation features (e.g., period, speed variation, spacing and headway) have not received quantitative analysis. This study conducts a set of field experiments designed to inspect such relationships. In these experiments, 12 vehicles equipped with high-resolution global positioning system (GPS) devices following one another on public roads, and the lead vehicle was asked to move with designed trajectory profiles incorporating various parameters. Measurements of five features are extracted from processing the field vehicle trajectory data with a time-domain method. Frequency analysis is also proposed with the Fourier transform method to verify the effectiveness of the features measured by the time-domain method. Compared to the frequency-domain method, the time-domain method yields more measurements with comparable quality and is more robust on trajectories with a small number of oscillation cycles. Then, a series of linear regression analyses reveal a number of new findings on the relationships between these features. For example, the time gap between two consecutive vehicles is negatively correlated with the speed standard deviation of the preceding vehicle and the initial speed of the following vehicle. It is also positively correlated with the average speed of the preceding vehicle and the initial spacing. The findings are helpful in constructing new microscopic traffic models better describing traffic oscillation dynamics. To illustrate this benefit, revised car following models are proposed to capture the relationship between time gap and other features. The simulation results show that the revised models yield better prediction accuracy (in range of 18% to 40% with the oscillation experiment dataset and in range of 30% to 63% with the stationary experiment dataset) than the classical models on reproducing real-world trajectories.

Keywords: Traffic oscillation, field experiments, high-resolution GPS devices, empirical analysis, car-following model.

1. Introduction

Traffic oscillation, also called “stop-and-go” traffic, causes traffic congestion, capacity drop, travel delay, safety hazards and excessive fuel consumption and emissions. The dynamics and impacts of traffic oscillation depend on multiple features of traffic oscillation, including period, amplitude, time gap, spacing, headway, etc. A great number of theoretical models and empirical studies have been conducted in the past several decades to investigate traffic propagation mechanisms via measuring and modeling some of these features.

A variety of theoretical models have been developed to reproduce the properties of traffic oscillation. In microscopic traffic, numerous car-following models were proposed to describe the relationships between two consecutive vehicles and to play a vital role in capturing traffic oscillation propagation. Representative models include the linear General Motor (GM) model (Chandler et al. 1958; Herman et al. 1959), Newell’s model (Newell 1961), Gipps’ model (Gipps 1981), the optimal velocity model (OVM) (Bando 1995) and the

* Corresponding author.
Tel: +1(813) 974-2275 (Xiaopeng Li); Fax: +1(813)974-2957 (Xiaopeng Li); E-mail: yaohhddong@163.com (Handong Yao), xiaopengli@usf.edu (Xiaopeng Li).

intelligent driver model (IDM) (Treiber et al. 2000). Noteworthy most of relevant studies used analytical modeling or numerical simulation rather than field experiments due to the lack of precise field data. Papageorgiou (1998) also mentioned that traffic oscillation cannot reveal all of its mystery without the parameters estimation against field data.

With the existence of precise field data, some studies focused on calibrating existing car-following models (Rakha and Crowther 2003; Treiber and Kesting 2012; Rhoades et al. 2016; Zhang et al. 2018) or proposing new car-following models considering traffic oscillation (Laval et al. 2014; He et al. 2015; Tian et al. 2016b; Treiber and Kesting 2017; Zhou et al. 2017). Other studies focused on extracting and measuring oscillation characteristics (Zielke et al. 2008; Yeo and Skabardonis 2009; Li et al. 2010, 2012, 2014, 2018, Chen et al. 2012, 2014, Jiang et al. 2014, 2015; Sun 2014; Tian et al. 2016a; Saifuzzaman et al. 2017) and investigating traffic oscillation propagation due to driver behaviors (Ahn and Cassidy 2007; Laval et al. 2007; Zheng et al. 2011a; Oh and Yeo 2015). Among these studies, the most common data were from loop detectors (Zielke et al. 2008; Li et al. 2010; Zheng et al. 2010, 2011b; Treiber and Kesting 2012) and cameras (e.g., NGSIM data) (Knoop et al. 2008; Yeo and Skabardonis 2009; Laval and Leclercq 2010; Zheng et al. 2011a; Laval 2011; Li et al. 2012, 2014, Chen et al. 2012, 2014; Oh and Yeo 2015; Fernandez et al. 2017; Saifuzzaman et al. 2017). The data used in these studies were, however, limited within short road segments that could not reflect the dynamics of traffic flow along a long travel distance. And prevailing errors in the dataset may compromise microscopic driving behavioral models (Coifman and Li 2017). Recently, with the development of the global positioning system (GPS), researchers started to use high-resolution GPS devices to collect data (Jiang et al. 2014, 2015; Tian et al. 2016a; Li et al. 2018). They collected high resolution trajectory data for each instrumented vehicle for a long travel period and distance, which contains rich information on the advent and propagation of traffic oscillation. These recent studies mainly focused on only a subset of oscillation features such as speed variance, average speed and spacing, yet did not comprehensively address other features such as oscillation periods and time gaps. Further, the relationships between traffic oscillation features have not yet received quantitative analysis.

Despite these fruitful findings, however, it is necessary to inspect all relevant traffic oscillation features and quantifying their relationships to fully understanding the mechanisms and impacts of traffic oscillation. For example, oscillation period is largely resulted from driving behavior and traffic dynamics (Li and Ouyang 2011), and causes driving uncomfortable due to repeated acceleration and declaration cycles. Time gap is closely related to drivers' reaction time and vehicle dynamics, and determines spatial and temporal propagations of shock waves created from traffic oscillation. Further, these features are likely not independent, for example, Li et al. (2014, 2018) noticed that oscillation period increases as oscillation amplitude grows. Kesting et al. (2008) analyzed the relationships between traffic oscillation and reaction time, update time and adaptation time, and found that long-wavelength string instability is mainly driven by the adaptation time while short-wavelength local instabilities are related to update time and reaction time. These interesting issues, however, have seldom been quantitatively studied from a statistical point of view with field data. This hinders our capability of analyzing and modeling traffic oscillation, imposes knowledge gaps in effective managing traffic oscillation and mitigating its adversary impacts, and further makes improvement in traffic control and other engineering research and applications to eliminate negative effects of traffic oscillation (Aboudina et al. 2016; Arshi et al. 2018; Saxena et al. 2019).

Motivated by the above gaps, we conducted a set of field experiments with a platoon of 12 human driven vehicles on a 5-km-long highway section in Harbin, China. High-resolution GPS devices were mounted on the vehicles to record the detailed trajectory of each individual vehicle. Different from Jiang's experiments (Jiang et al. 2014), our experiments focus on the relationships between traffic oscillation features. In the proposed field experiments, the leading vehicle was asked to proceed in periodical acceleration and deceleration patterns with different oscillation parameters. Several features (e.g., period, average speed, speed standard deviation, time gap, initial speed and initial spacing) are extracted from the experiments to

investigate the propagation of traffic oscillation with a time-domain method. Frequency analysis is also proposed with the Fourier transform (FT) method to verify the effectiveness of the features measured by the time-domain method. Compared with the frequency-domain method, the time-domain method in general yields comparable measurements and is more robust on trajectory with a small number of oscillation cycles. Further, the time-domain method populates more measurements and thus is more suitable for statistical analyses investigating the relationships of traffic oscillation features. A number of new findings of the relationships between traffic oscillation features are presented. For example, the time gap to the preceding vehicle is positively correlated with the average speed of the preceding vehicle and the initial spacing, and negatively correlated with the speed standard deviation of the preceding vehicle and the initial speed of the following vehicle. Finally, to demonstrate the application of the extracted relationships, we apply the above findings to revise the classic car following models and validate significant improvement in its capacity on reproducing real-world trajectories.

The contributions of this paper are summarized as follows. 1) High-resolution GPS trajectory data are extracted from traffic oscillation field experiments, which provides a new dataset to calibrate and validate traffic flow models considering traffic oscillation. 2) A new time-domain method is proposed to extract traffic oscillation features and compared with a FT based frequency-domain method. 3) The relationships between traffic oscillation features and their implications to traffic oscillation development are captured through empirical analysis. 4) Revised car following models are proposed based on the time gap function from the empirical analysis, and the revised car following models show better performance than the classic car following models on reproducing field data. The findings from this study will advance our understanding on traffic oscillation mechanisms and impacts, and also provide fundamental formulas for developing more traffic-oscillation-aware models, strategies and policies for traffic control and management.

The rest of this paper is organized as follows. Section 2 states the experimental setup and results. In Section 3, traffic oscillation features are defined, and the method of processing data is described. Section 4 conducts linear regression on the features to analyze their relationships, and proposes revised car following models based on the findings from empirical analysis. Section 5 concludes this paper and briefly discusses future research directions.

2. Experimental Setup and Results

2.1. Experimental setup

The field experiments were implemented on October 24th, 2015. The experiment settings are summarized below.

Location: All experiments were carried out on a 5 km highway section of National Highway G202 (Lanxi direction) in Harbin, Heilongjiang, China. See Figure 1~~Figure 1~~ (a) for the map of the test road. The black curve depicts the road segment in Google Maps, and the blue arrows indicate the traffic moving direction. As is shown in Figure 1~~Figure 1~~ (b), there are no traffic lights on the test road. The test road is a bi-direction and four-lane highway. Note that national highway G202 is not a freeway, and the speed limit is 80 km/h. It allows vehicles to have a U-turn on the test road. The traffic is light on the test road so that the vehicle platoon is not disturbed by other vehicles. Further, with the cooperation of traffic polices, it is safe and legal to conduct a set of traffic oscillation field experiments on the test road.

Equipment: The vehicle platoon contained 12 vehicles with identical sizes and models (i.e., Kia K5). A high-resolution GPS device, called GPS-RTK based STAR-RTK-M9, was installed in each vehicle to collect field data (i.e., locations and speed). The data measurement errors of the GPS device are within ±1m for location and ±1km/h for speed. And the sampling frequency is 20Hz (i.e., the sampling time interval is 0.05s).

Configurations: Since the objective of the field experiments was to investigate the propagation of traffic oscillation and the relationships in traffic oscillation features, we conducted 12 experiments with different traffic oscillation parameter settings for the leading vehicle, as shown in Table 1~~Table 1~~. The cruise time

indicates the duration time of cruising. The acceleration and the maximum speed decide the adaptation time of traffic oscillation. And then, the time period of traffic oscillation consists of cruising time and adaptation time. The difference between the maximum and minimum speeds implies the magnitude of traffic oscillation. Basically, a leading vehicle driver was asked to periodically vary vehicle speed based on a profile specified by the parameters. Within each time period, the ideal leading vehicle speed profile would accelerate to the maximum speed with the designed acceleration rate, then cruise at the maximum speed, and finally decrease the speed to the minimum speed with a deceleration rate identical to the negation of the previous acceleration rate. Note that it is difficult for the leading vehicle driver to follow the perfect speed profile, and the driver was just asked to follow this profile as best as he/she can. Other drivers were told to follow the preceding vehicle as usual without overtaking. When approaching the end of the road segment, all GPS devices stopped collecting data, and the vehicle platoon made a U-turn and stopped. After all vehicles stopped, a new run of the experiment began, and the GPS devices restarted to collect data at the same time.

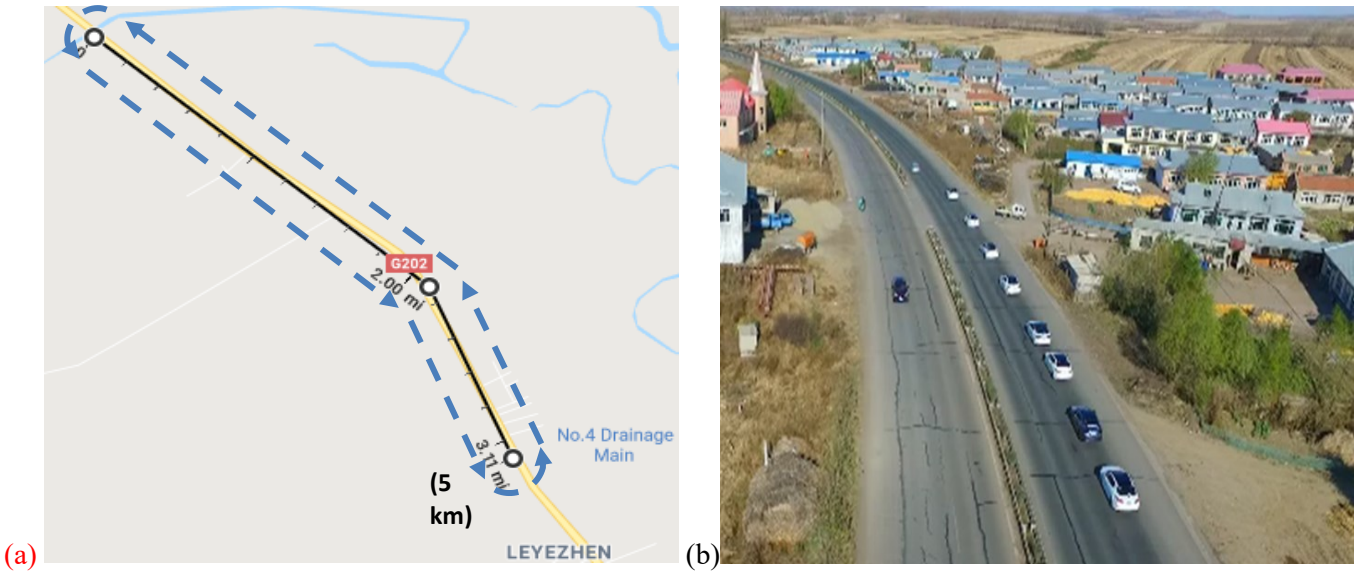

Figure 1 Experimental section of the field tests: (a) Road geometry in Google maps; (b) Actual experimental environment.

Table 1 Parameter settings for the leading vehicle in different experiments.

	Cruise time (s)	Designed acceleration (km/h/s)	Minimum speed (km/h)	Maximum speed (km/h)
Experiment 1	30	1	30	40
Experiment 2	30	2	30	40
Experiment 3	30	1	20	40
Experiment 4	30	2	20	40
Experiment 5	120	1	30	40
Experiment 6	120	2	30	40
Experiment 7	120	1	20	40
Experiment 8	120	2	20	40
Experiment 9	30	1	60	70
Experiment 10	30	2	60	70
Experiment 11	30	1	50	70
Experiment 12	30	2	50	70

Figure 2~~Figure 2~~ illustrates an ideal speed trajectory with parameters setting. The pre-designed cruise is 30s. The maximum speed, marked by red dashed line, is 40km/h. The minimum speed is 20km/h. And the acceleration is shown by the slope as 2km/h/s.

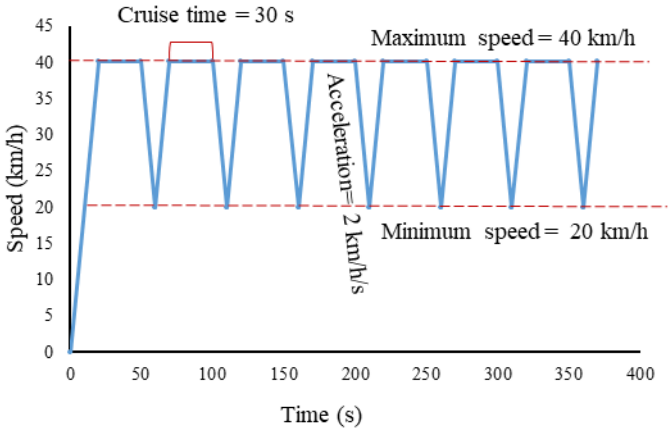

Figure 2 An example of ideal speed trajectory with the parameter settings.

2.2. Field test results

Figure 3~~Figure 3~~ shows an example of time-location trajectories of the test vehicles from one experiment. There are some missing data due to the errors of GPS (e.g., vehicle was beneath a bridge or GPS was loss of signal). Thus, we will use interpolation to recover the time-location trajectories in Section 3. In Figure 3~~Figure 3~~, we find that there exist frequent traffic oscillations through the 5km road section, which follow the experiment settings. The detailed oscillatory series of time-space trajectories can be found in Figure 5~~Figure 5~~ (a).

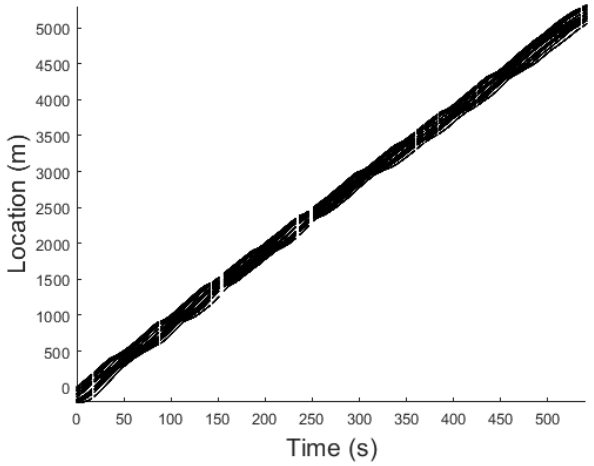

Figure 3 An example of time-space trajectories of the test vehicles.

Figure 4~~Figure 4~~ shows an example of time-speed trajectories of the 1st, 2nd and 10th vehicles. The blue-square curve, the black-circle curve and the red-triangle curve plot the time-speed trajectories of the 1st, 2nd and 10th vehicles, respectively. And the blue-dotted line shows the average speed of the first vehicle. We find the operation of the leading vehicle (i.e., the 1st vehicle). The cruise time is around 30s. The maximum speed is a little higher than 40km/h, and the average speed is around 35-40km/h, and the minimum speed is about 20km/h. This leading vehicle's speed trajectory is similar as the ideal leading vehicle's speed trajectory in Figure 2~~Figure 2~~. That means the speed fluctuation of the leading vehicle is in general consistent with the pre-set parameters. Further, it is clear that the speed trajectory fluctuates more abruptly from the leading vehicle to the 10th vehicle. And there exists a shift time between two consecutive vehicles so that the speed trajectory of the 10th vehicle is hysteretic compared with the 1st and 2nd vehicles. This indicates that traffic oscillation propagates with varying traffic oscillation features from the leading vehicle to the last vehicle.

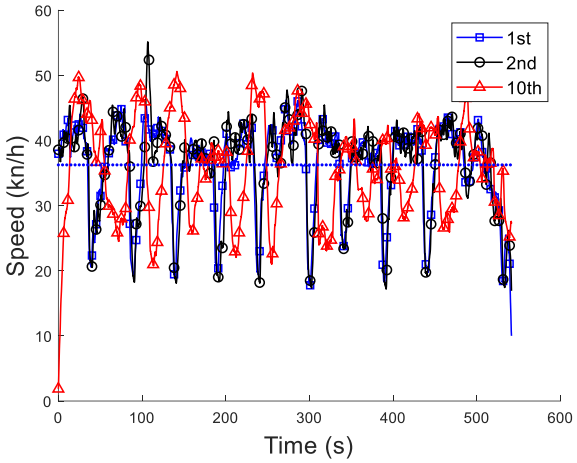

Figure 4 An example of time-speed trajectories of the 1st, 2nd and 10th vehicles.

3. Feature Measurements and Data Processing

For the convenience of readers, the key notation is summarized in the Appendix A.

3.1. Notation

For the convenience of describing traffic oscillation features, following notation is given.

Time: Consider a set of time indexed by $t = 0, \Delta t, 2\,\Delta t, \dots, T$, where Δt is the sampling time interval and T is the maximum time. Let $\mathbf{T} \coloneqq \{0, \Delta t, 2\,\Delta t, \dots, T\}$ denote the set of time.

Traffic oscillation pre-set cycle: Traffic oscillation pre-set cycles are indexed by $k = 1,2, \dots, K$, where $K = \lfloor T/tp^{pre} \rfloor$ is the maximum pre-set cycle number. The length of one traffic oscillation pre-set cycle is $tp^{pre} = tc^{pre} + 2 \times \left\lfloor \frac{vv^{pre}}{a^{pre}} \right\rfloor$, where tc^{pre} is the pre-designed cruise time, vv^{pre} is the pre-designed speed variation range, and a^{pre} is the pre-designed acceleration.

Vehicle: Consider a platoon of vehicles indexed by $n = 1,2, \dots, N$. Let $\mathbf{N} \coloneqq \{1,2, \dots, N\}$ denote the set of vehicles.

Location: Let $x_n(t)$ denote the location of vehicle $n \in \mathbf{N}$ at time $t \in \mathbf{T}$.

Speed: Let $v_n(t)$ denote the speed of vehicle $n \in \mathbf{N}$ at time $t \in \mathbf{T}$. To make consistency with location with meters as unit, the unit of speed is set as m/s. Thus, 40km/h is about 11.11m/s, and 70km/h is about 19.44m/s.

Acceleration: Let $a_n(t)$ denote the acceleration of vehicle $n \in \mathbf{N}$ at time $t \in \mathbf{T}$.

3.2. Feature measurements

In order to measure the duration time and magnitude of traffic oscillation, time period, average speed, and speed standard deviation are utilized.

Time period (tp): Let $tp_{nk} = t^v_{n(k+1)} - t^v_{nk}$ denote the cycle length of vehicle $n \in \mathbf{N}$ in traffic oscillation pre-set cycle $k \in \mathbf{K}$. $t^v_{nk} = argmin_{t \in \mathbf{T}_k} v_n(t)$ is the time point of the local minimum speed of vehicle $n \in \mathbf{N}$ in traffic oscillation pre-set cycle $k \in \mathbf{K}$. And δ_k is the time interval to search local minimum speed in pre-set cycle k. Once we find a t^v_{nk} with the global minimum speed $argmin_{t \in \mathbf{T}} v_n(t)$, the current traffic oscillation pre-set cycle is set as $k = \lfloor t^v_{nk}/tp^{pre} \rfloor$. Then, $t^v_{n(k+1)}$ is calculated by forward searching in time interval $\delta_{k+1} \in \left[t^v_{nk} + tp^{pre}/2\,,\, t^v_{nk} + 3tp^{pre}/2\right]$, and $t^v_{n(k-1)}$ is calculated by backward searching in time interval $\delta_{k-1} \in \left[t^v_{nk} - 3tp^{pre}/2\,,\, t^v_{nk} - tp^{pre}/2\right]$. With this, let $p \in \mathbf{P} = [1,2, \dots, P]$ denote the index of time period, where $P = K - 1$. The time period length of vehicle $n \in \mathbf{N}$ in period $p \in \mathbf{P}$ is $tp_{np} = tp_{nk}$. And the time interval in period $p \in \mathbf{P}$ of vehicle $n \in \mathbf{N}$ is $\delta_{np} \coloneqq \left[t^v_{nk}, t^v_{n(k+1)}\right]$. Let $I_{np} = tp_{np} \times f$ denote the

number of data points of vehicle $n \in \mathbf{N}$ in period $p \in \mathbf{P}$, where $f = 1/\Delta t$ is the sampling frequency. See Figure 6~~Figure 6~~, the time interval between two consecutive local minima (i.e., black circles or red triangles). This reflects the duration time that traffic oscillation takes in one complete cycle.

Average speed (vmn): Let $vmn_{np} = \frac{1}{I_{np}} \sum_{t \in \delta_{np}} v_n(t)$ denote the average speed of vehicle $n \in \mathbf{N}$ in period $p \in \mathbf{P}$.

Speed standard deviation (vsd): Let $vsd_{np} = \sqrt{\sum_{t \in \delta_{np}} \left(v_n(t) - vmn_{np}\right)/I_{np} - 1}$ denote the speed standard deviation of vehicle $n \in \mathbf{N}$ in period $p \in \mathbf{P}$ to reflect the magnitude of traffic oscillation.

In addition, we add other features, average time gap and initial speed and spacing to measure the trajectory shifting happened in time-speed trajectories.

Time gap (tg): Let $tg_{np} = argmin_{t \in \delta_{np}} v_n(t) - argmin_{t \in \delta_{np}} v_{n-1}(t)$ denote the time interval that speed traffic oscillation travels from vehicle $n-1 \in \mathbf{N}$ to vehicle $n \in \mathbf{N}$ in period $p \in \mathbf{P}$. See Figure 6~~Figure 6~~, the time gap is marked as the time interval between the minima of the first vehicle (i.e., black circles) and its neighbor minima of the second vehicle (i.e., red triangles).

Initial speed (vin): Let $vin_{np} = v_{np}\left(t_{nk}^{v}\right)$ denote the speed of vehicle $n \in \mathbf{N}$ at the beginning of period $p \in \mathbf{P}$.

Initial spacing (sin): Let $sin_{np} = s_{np}\left(t_{nk}^{v}\right)$ denote the spacing of vehicle $n \in \mathbf{N} \backslash \{1\}$ at the beginning of period $p \in \mathbf{P}$.

3.3. Data processing

To obtain all oscillation features from the raw field data, we need to do a series of data processing.

Step 1: Selecting a suitable time interval for each experiment. In order to get more complete cycles of traffic oscillation for all vehicles, we need to select a suitable time set **T** for each experiment.

Step 2: Smoothing trajectory for every vehicle in all experiments. Before smoothing, linear interpolation method is applied to fixed missed data on location trajectories. Then, we extract macroscopic series (black dashed line in Figure 5~~Figure 5~~ (a)) and oscillatory series (blue dash-dot line in Figure 5~~Figure 5~~ (a)) from original location trajectories (red solid line in in Figure 5~~Figure 5~~ (a)) according to the method in Li's work (2012). Next, moving average method is applied to smooth oscillatory series trajectories so that we can eliminate unnecessary noises. Then, smoothed speeds $\{\tilde{v}_n(t)\}_{t \in \mathbf{T}}$ and accelerations $\{\tilde{a}_n(t)\}_{t \in \mathbf{T}}$ are recalculated according to the smoothed trajectories (red solid line in Figure 5~~Figure 5~~ (b)).

Step 3: Finding time periods on smoothed trajectories. Here, we separate a smoothed speed trajectory into several parts (i.e., set of traffic oscillation pre-set cycles **K**) according to the pre-designed cruise time and adaptation time. After that, we plan to find every time period tp_{nk}, $\forall n \in \mathbf{N}, k \in \mathbf{K}$ in measured time intervals. First, the key to find time periods is to find the lowest speed points among a speed trajectory of the first vehicle. See Figure 6~~Figure 6~~, it illustrates an example of all local lowest speed points (i.e., black circles for 1st vehicle and red triangles for 2nd vehicle) among speed trajectories. And the point marked by a bigger black circle is the global lowest speed point of the first vehicle. Then, forward searching and backward searching with a pre-set time period (e.g., tp^{pre}= 35s, 40s, 50s, 125s, 130s or 140 s in these experiments) are applied to find other local lowest speed points of the first vehicle within searching intervals, marked by black circles in Figure 6~~Figure 6~~. For the following vehicles (e.g., 2nd vehicle), the local lowest speed points (i.e., red triangles) are picked in the time periods of the first vehicle. In general, they are in the neighborhood of the first vehicle's local lowest speed points. And the time intervals between two consecutive local lowest speed points are denoted as time periods. For example, there are 8 local lowest points in Figure 6~~Figure 6~~. Thus, we collect 7 time periods among this speed trajectory.

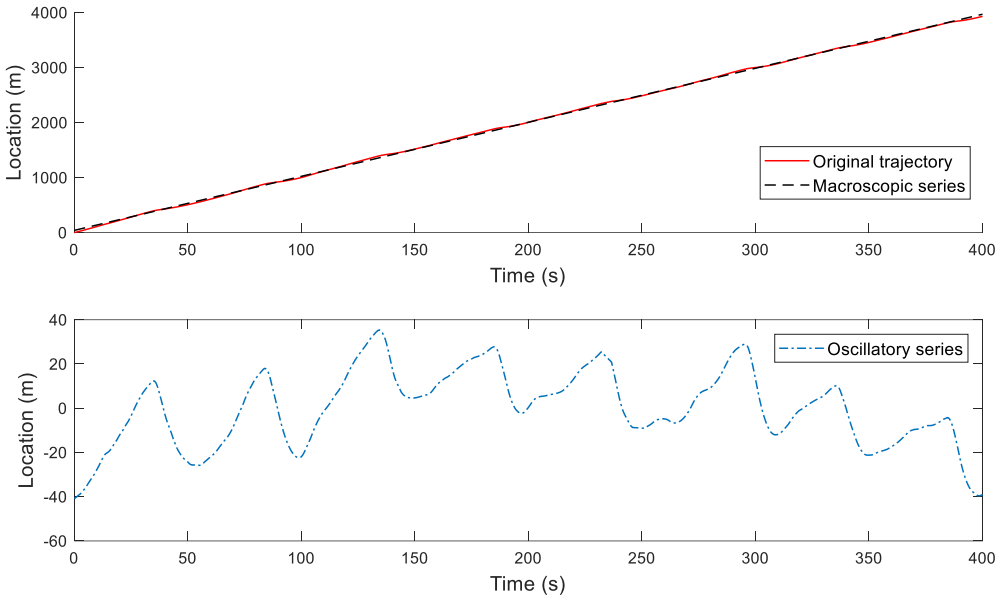

(a)

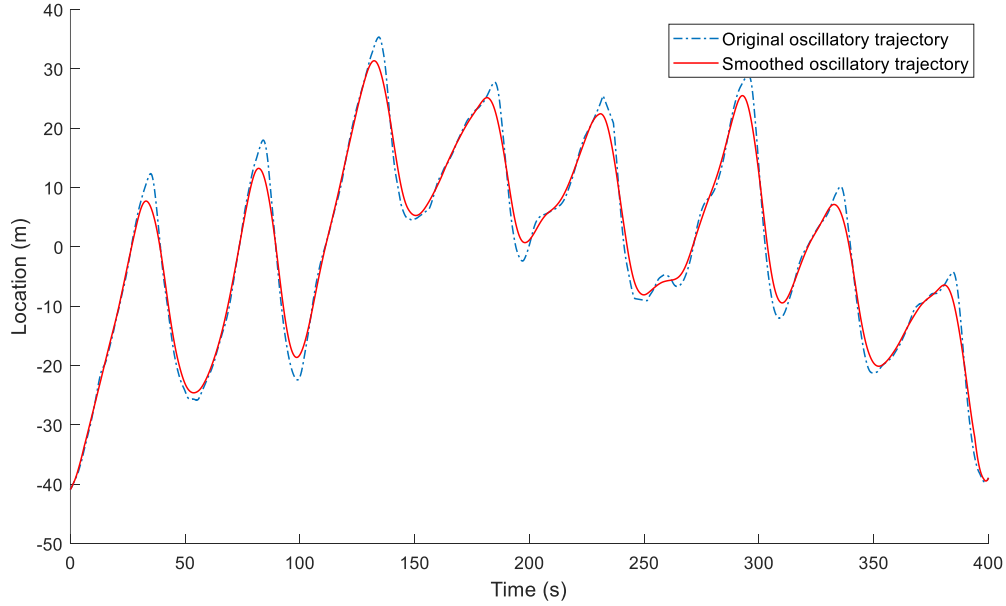

(b)

Figure 5 An example of trajectory smoothing: (a) Extract macroscopic series and oscillatory series from the original trajectory; (b) Smooth oscillatory series trajectory.

Step 4: Calculating all the other features (i.e., sin_{np}, vin_{np} vmn_{np}, tg_{np} and vsd_{np}) related to the above measured time periods (i.e., tp_{np}). Each feature contains 7 data points according to 7 measured time periods.

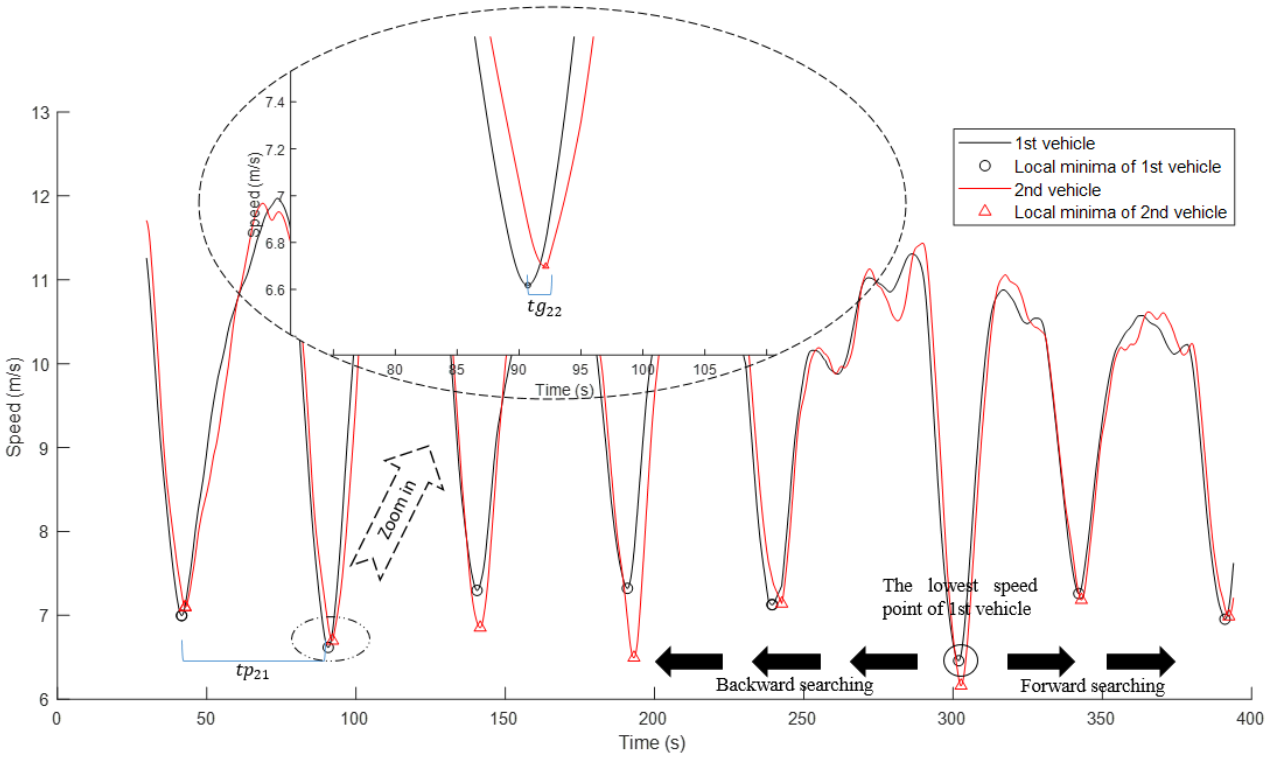

Figure 6 An example of finding all time periods.

3.4 Frequency analysis

To verify the above features measured by the time-domain method, a proven and simple implementable method, called the Fourier Transform (FT) based frequency-domain method proposed by Li et al. (2012), is used to capture the dominant frequency set $\{\Omega_n\}_{n\in\mathbf{N}}$ for comparison with the above time-domain measurements.

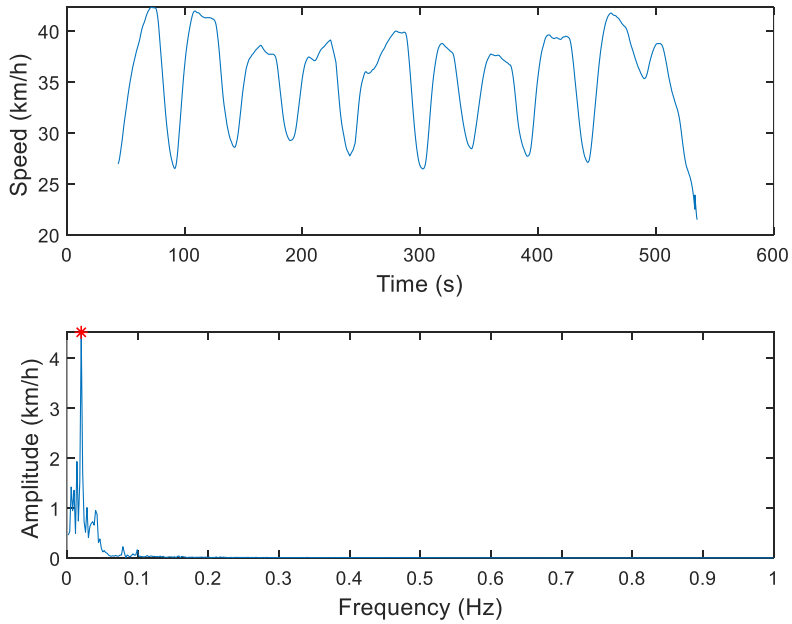

Figure 7 An illustration of a time-speed trajectory and the corresponding FT spectrum in case 1.

The dominant frequency set is calculated as follows,

$$\Omega_n = \text{argmax}_{\Omega} \int_{\mathbf{T}} \left| \tilde{v}_n(t) e^{-j\Omega t} \right| dt, \quad (1)$$

where $j = \sqrt{-1}$, $e \approx 2.718$, Ω_n is the dominant frequency of vehicle n and $\tilde{v}_n(t)$ is the smoothed speed of vehicle n at time $t \in \mathbf{T}$.

The upper subfigure in Figure 7~~Figure 7~~ shows a time-speed trajectory in case 1. It is found the average time period is about 50 s. The lower subfigure in Figure 7~~Figure 7~~ shows the corresponding FT spectrum in case 1. There is an obvious peak, marked by red star, in the FT spectrum at about 0.0203 Hz, which is also referred as the dominant frequency. Thus, the corresponding dominant period as the invers of the dominant frequency is about 49.26 s, which is almost the same as the time period measured in the time-domain method. This verifies that the proposed time-domain method is effective on measuring oscillation features.

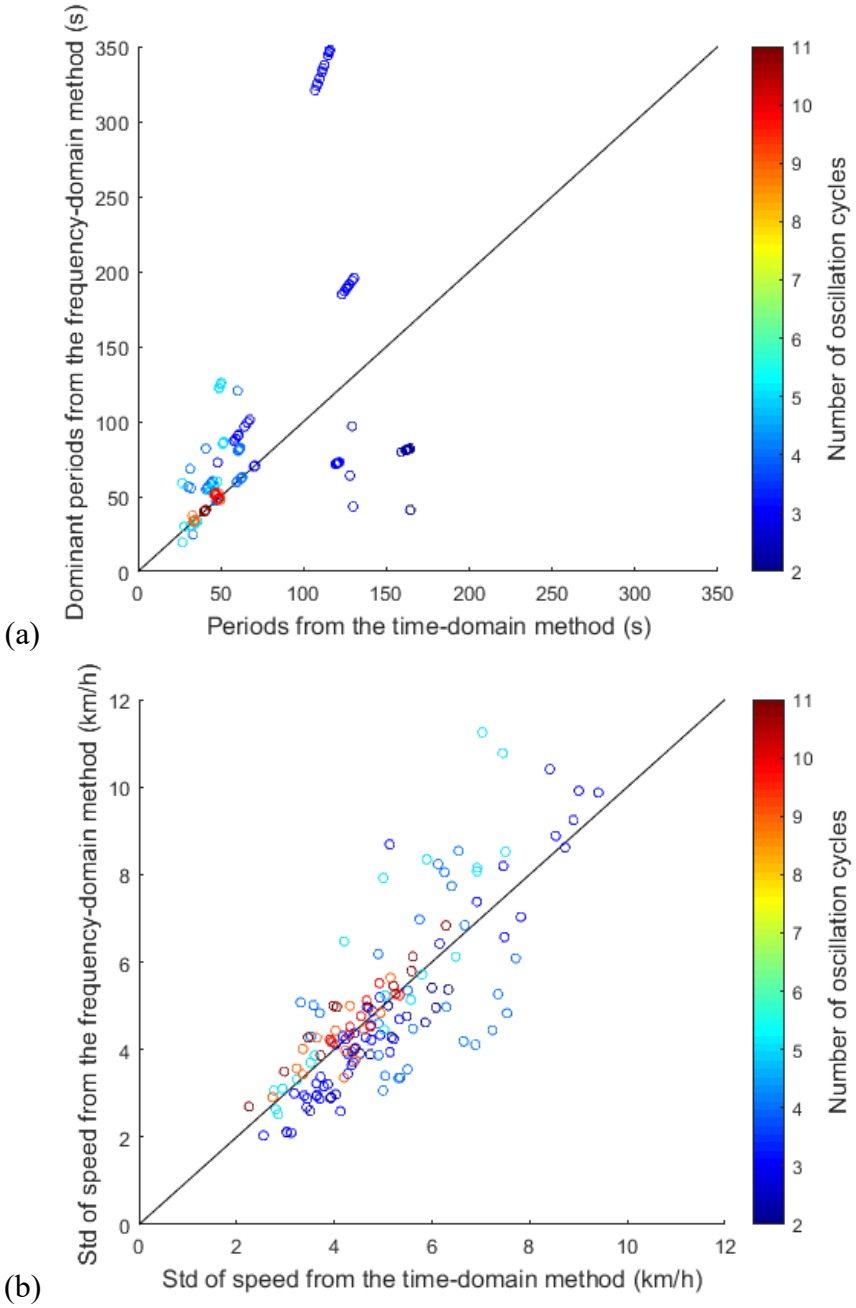

Figure 8 The comparison results between the time-domain method and the frequency-domain method: (a) time period; (b) speed standard deviation.

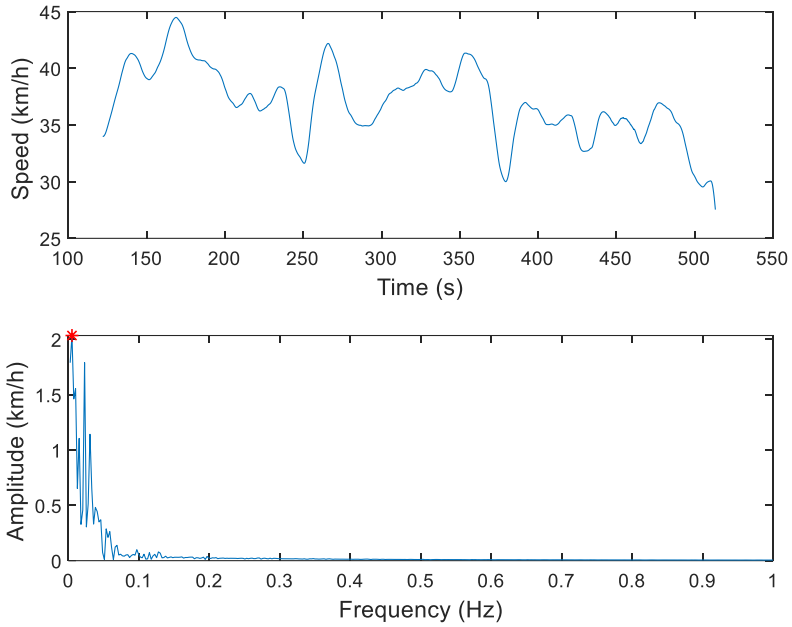

Figure 9 An illustration of a time-speed trajectory and the corresponding FT spectrum in case 2.

Figure 8~~Figure 8~~ shows the comparison results between the time-domain method and the frequency-domain method considering the number of oscillation cycles. Compared with the frequency-domain method, the time-domain method has comparable results on measuring periods and speed standard deviations. However, when the number of oscillation cycles is small, the dominant periods measured by the frequency-domain method become more fluctuating due to zero padding, and thus the corresponding comparison data points considerably deviate from the 45 degree line. For example, in Figure 9~~Figure 9~~, the time-speed trajectory shows that the average time period is about 130.4 s with 3 oscillation cycles. While the FT spectrum shows the dominant period is 195.6 s. Further, the time-domain method considering each individual oscillation cycle captures more data points than the frequency-domain method considering several oscillation cycles. Thus, the oscillation features with more data points measured by the time-domain method are used in the following empirical analysis to yield a better performance on investigating the relationships of these features.

4. Empirical Analysis and Revised Car Following Models

4.1. Empirical analysis with linear regression methods

To investigate the relationships of the traffic oscillation features between the preceding vehicle and the following vehicle, linear regression approach is used to analyze the measured features in Section 3 with R language. For the consistency of variables naming in R language, we use $var.p = \{var_{np}\}_{n\in\mathbf{N}\setminus\{N\},p\in\mathbf{P}}$ and $var.f = \{var_{np}\}_{n\in\mathbf{N}\setminus\{1\},p\in\mathbf{P}}$ to denote the feature sets of the preceding vehicle and the following vehicle, respectively. For example, $tp.p = \{tp_{np}\}_{n\in\mathbf{N}\setminus\{N\},p\in\mathbf{P}}$ denotes the set of the time period lengths of the preceding vehicle, and $tp.f = \{tp_{np}\}_{n\in\mathbf{N}\setminus\{1\},p\in\mathbf{P}}$ denotes the set of the time period lengths of the following vehicle. The detailed definitions of these variables are summarized in Appendix A.

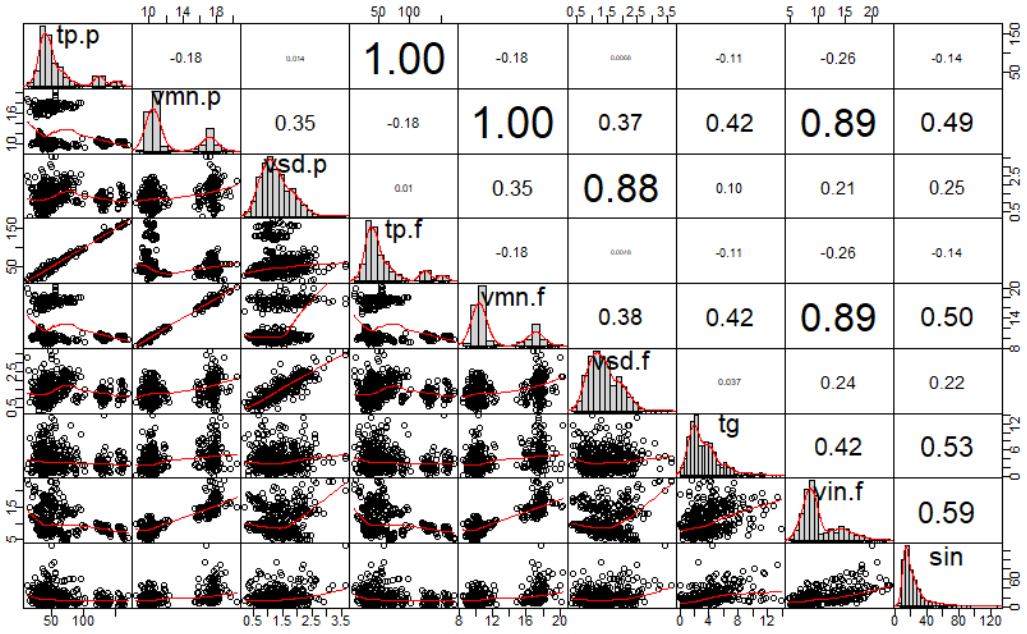

Figure 10 The correlations among all features.

Then, we check the relationships among all features (i.e., $tp.p$, $vmn.p$, $vsd.p$, $tp.f$, $vmn.f$, $vsd.f$, tg, sin and $vin.f$) by plotting the correlation matrix and calculating the correlation coefficients between each two features. See Figure 10~~Figure 10~~, some of the scatter diagrams have two classifications. This is because of the settings of field experiments (i.e., two kinds of time periods and two kinds of maximum speeds). We find that there exist linear relationships between the same features of the preceding vehicle and the following vehicle, e.g. the correlation between $tp.p$ and $tp.f$. This shows the truth of car-following behavior. And there exists a linear relationship between $vmn.f$ and $vin.f$. However, the linear correlations among other features are not obvious with small correlation coefficients. In order to explore more detailed relationships in traffic oscillation features, we conduct a set of linear regression tests using tg, $tp.f$, $vmn.f$, and $vsd.f$ as dependent variables, respectively.

Table 2 Linear Regression Result Using $vmn.f$ as Dependent Variable.

	Estimate	Std. Error	t value	Pr(> |t|)	Significance
(Intercept)	-0.0153	0.0368	-0.417	0.677	
$vmn.p$	0.9935	0.0033	297.932	<2e-16	***
$vin.f$	0.0046	0.0007	6.077	2.3e-09	***

Residual standard error: 0.2233 on 547 degrees of freedom. Multiple R-squared: 0.9954, Adjusted R-squared: 0.9954. F-statistic: 8.948e+04 on 2 and 544 DF, p-value: < 2.2e-16.

Table 2~~Table 2~~ shows the regression result using $vmn.f$ as the dependent variable. We find that $vmn.f$ is strongly linear correlated with independent variables ($vmn.p$ and $vin.f$) with all t-statistic values above 6 and great goodness of fit with a high adjusted R-squared of 0.9954. As shown in Table 2~~Table 2~~, $vmn.p$ shows a strong positive correlation with $vmn.f$. This follows the car-following laws and means that the average speed of the following vehicle is almost the same as the preceding vehicle. The significant linear relationship between $vmn.f$ and $vmn.p$ can be also found in Figure 10~~Figure 10~~. Thus, the linear relationship of $vmn.f$ and the significant independent variables is formulated as follows,

$$vmn.f = 0.9935vmn.p + 0.0046vin.f. \quad (2)$$

Table 3 Linear Regression Result Using $vsd.f$ as Dependent Variable.

	Estimate	Std. Error	t value	Pr(> |t|)	Significance
(Intercept)	0.0723	0.0441	1.64	0.1015	
$vmn.p$	0.0131	0.0036	3.66	0.0003	***
$vsd.p$	0.8785	0.0219	40.15	<2e-16	***

Residual standard error: 0.2567 on 547 degrees of freedom. Multiple R-squared: 0.7822, Adjusted R-squared: 0.7814. F-statistic: 982 on 2 and 547 DF, p-value: < 2.2e-16.

Table 2 shows the regression result using $vmn.f$ as the dependent variable. We find that $vmn.f$ is strongly linear correlated with independent variables ($vmn.p$ and $vin.f$) with all t-statistic values above 6 and great goodness of fit with a high adjusted R-squared of 0.9954. As shown in Table 2, $vmn.p$ shows a strong positive correlation with $vmn.f$. This follows the car-following laws and means that the average speed of the following vehicle is almost the same as the preceding vehicle. The significant linear relationship between $vmn.f$ and $vmn.p$ can be also found in Figure 10. Thus, the linear relationship of $vmn.f$ and the significant independent variables is formulated as follows,

$$vmn.f = 0.9935vmn.p + 0.0046vin.f. \quad (2)$$

Table 3~~Table 3~~ shows the linear regression result using $vsd.f$ as the dependent variable. The adjusted R-squared value is 0.7814 indicating acceptable goodness of fit. Two independent variables are statistically significant with t-statistic values above 3. And we find $vsd.p$ is highly positively correlated with $vsd.f$ due to the car-following behavior. Besides, the average speed of the preceding vehicle provides a positive effect on $vsd.f$, which means that a higher speed will cause a sharper speed fluctuation. Therefore, the linear relationship of $vsd.f$ is formulated as follows,

$$vsd.f = 0.0131vmn.p + 0.8785vsd.p. \quad (3)$$

Table 4 Linear regression result using $tp.f$ as a dependent variable.

	Estimate	Std. Error	t value	Pr(> |t|)	Significance
(Intercept)	-0.0515	0.7188	-0.072	0.9429	
$tp.p$	0.9977	0.0044	226.129	<2e-16	***
$vmn.p$	0.3857	0.1106	3.486	0.0005	***
$vsd.p$	-0.7144	0.3229	-2.212	0.0273	*
sin	-0.3772	0.1028	-3.669	0.0003	***

Residual standard error: 3.619 on 544 degrees of freedom. Multiple R-squared: 0.9904, Adjusted R-squared: 0.9903. F-statistic: 1.117e+04 on 5 and 544 DF, p-value: < 2.2e-16.

The linear regression result using $tp.f$ as the dependent variable is shown in Table 2 shows the regression result using $vmn.f$ as the dependent variable. We find that $vmn.f$ is strongly linear correlated with independent variables ($vmn.p$ and $vin.f$) with all t-statistic values above 6 and great goodness of fit with a high adjusted R-squared of 0.9954. As shown in Table 2, $vmn.p$ shows a strong positive correlation with $vmn.f$. This follows the car-following laws and means that the average speed of the following vehicle is almost the same as the preceding vehicle. The significant linear relationship between $vmn.f$ and $vmn.p$ can be also found in Figure 10. Thus, the linear relationship of $vmn.f$ and the significant independent variables is formulated as follows,

$$vmn.f = 0.9935vmn.p + 0.0046vin.f. \quad (2)$$

Table 3 shows the linear regression result using $vsd.f$ as the dependent variable. The adjusted R-squared value is 0.7814 indicating acceptable goodness of fit. Two independent variables are statistically significant

with t-statistic values above 3. And we find $vsd.p$ is highly positively correlated with $vsd.f$ due to the car-following behavior. Besides, the average speed of the preceding vehicle provides a positive effect on $vsd.f$, which means that a higher speed will cause a sharper speed fluctuation. Therefore, the linear relationship of $vsd.f$ is formulated as follows,

$$vsd.f = 0.0131vmn.p + 0.8785vsd.p. \quad (3)$$

Table 4~~Table 4~~. There is a strong linear correlation between $tp.f$ and independent variables with all t-statistic values higher than 2.2 and a goodness of fit with an adjusted R-squared value of 0.9903. We find that $tp.f$ has a strong and positive correlation with $tp.p$. which has a much higher t-value than other independent variables. This implies that the time period length of the preceding vehicle has a drastically strong linear relationship with the time period length of the following vehicle. Figure 10~~Figure 10~~ also shows the linear relationship between $tp.p$ and $tp.f$. This makes the time period length maintain almost the same from the first vehicle to the last vehicle. Further, $tp.f$ is also positively correlated with $vmn.p$ and $vin.f$. It is possible that higher average speed and initial speed of the preceding vehicle cause a higher average speed of the following vehicle, this means the following vehicle is less likely to accelerate and then decelerate that much compared with vehicles with lower average speed. This is to say that the following vehicle's trajectory tends to be smoother with a longer oscillation period. Additionally, $tp.f$ is negatively correlated with $vsd.p$ and sin. This is probably because a higher speed standard deviation of the preceding vehicle causes a higher speed standard deviation of the following vehicle, which means the following vehicle's trajectory becomes unsmooth with a smaller oscillation period. As for the initial spacing, a lager initial spacing will cause a lager average spacing so that the driver of the following vehicle tends to accelerate to catch up then decelerate until at least the safety distance is guaranteed. This will result in a smaller oscillation period. According to the linear regression result, we formulate $tp.f$ as follows

$$tp.f = 0.9977tp.p + 0.3857vmn.p - 0.7144vsd.p - 0.3772sin + 0.0326vin.f. \quad (4)$$

As shown in **Error! Not a valid bookmark self-reference.**~~Table 5~~, it shows the linear regression result using tg as the dependent variable. We find tg has a weak linear relationship with $vmn.p$, $vsd.p$, sin and $vin.f$ due to the low adjusted R-squared value (i.e., 0.3243). The average time gap is strongly and positively correlated with the average speed of the preceding vehicle. This is because that drivers need more time to react when speed becomes higher. In addition, tg is significantly and positively correlated with sin. It is because a longer initial spacing may cause a longer average spacing and consequentially a longer time gap. Further, there is a significant negative correlation between the speed standard deviation of the preceding vehicle and the average time gap. This is probably that the following vehicle would react fast (i.e., time gap decreases) when the speed fluctuation increases. And $vin.f$ has a negative correlation with tg. Because a higher initial speed of the following vehicle leads to a greater average spacing, the average time gap is longer. Finally, the formulation of tg is shown as follows

$$tg = 0.2909vmn.p - 0.5173vsd.p + 0.0769sin - 0.1272vin.f. \quad (5)$$

Table 5 Linear Regression Result Using tg as Dependent Variable.

	Estimate	Std. Error	t value	Pr(> |t|)	Significance
(Intercept)	0.4299	0.3371	1.275	0.2027	
$vmn.p$	0.2909	0.0579	5.020	7.02e-17	***
$vsd.p$	-0.5173	0.1697	-3.047	0.00242	**
sin	0.0769	0.0071	10.752	< 2e-16	***
$vin.f$	-0.1272	0.0530	-2.400	0.0167	*

Residual standard error: 1.904 on 545 degrees of freedom. Multiple R-squared: 0.3292, Adjusted R-squared: 0.3243. F-statistic: 66.87 on 4 and 545 DF, p-value: < 2.2e-16.

Although, the adjusted R-squared value is not large. We compare the fitted time gap values from Equation

(5)~~(5)~~ (i.e., the red solid curve) and the actual observations (i.e., the dashed black curve) in Figure 11~~Figure 11~~, and find that these results are in general consistent, though the observed data are heavier on the extreme values. This could be because noises and errors in measurements may amplify time gap variations.

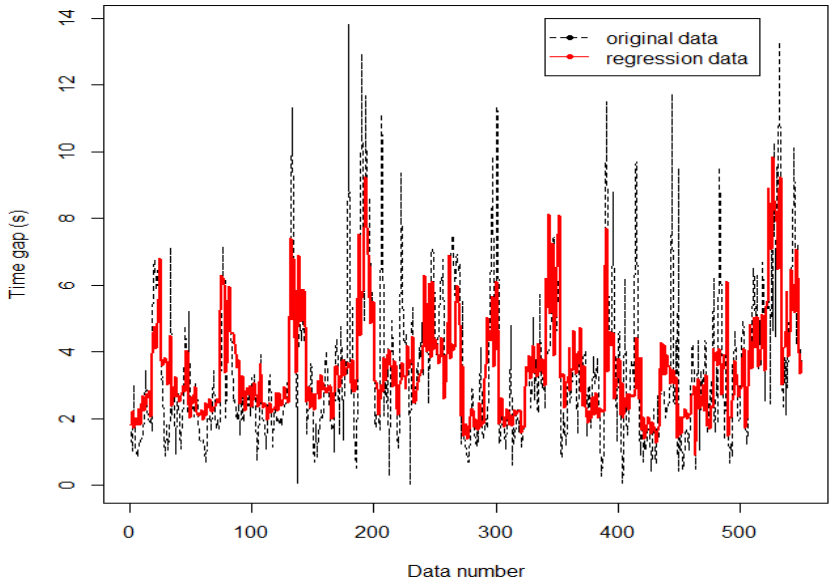

Figure 11 Regression results of time gap.

After linear regression analysis, empirical analysis results are summarized as follows.

1) The initial spacing is positively correlated with the average spacing and time gap, and negatively correlated with the time period length of the following vehicle. It is found that a traffic oscillation starting with a long initial spacing can cause a long average spacing and a long time gap. Thus, it will shorten the oscillation period of the following vehicle.

2) The initial speed of the following vehicle is negatively correlated with the average spacing and time gap, and positively correlated with the average speed and time period length of the following vehicle. A traffic oscillation starting with a low initial speed leads to a large average spacing and a long time gap. This results in a lower average speed and lower time period due to less range of speed than can be accelerated.

3) The average speed and the time period length of the following vehicle are highly and positively correlated with the average speed and the time period length of the preceding vehicle, respectively. This reflects the fact the average speed and time period length maintain almost the same from the first vehicle to the last one.

4) The speed standard deviation of the following vehicle is positively correlated with the average speed and speed standard deviation of the preceding vehicle. It shows that the speed is amplified from the first vehicle to the last one.

Among these findings, while 3) and 4) are consistent with classic traffic flow models, 1) and 2) add new knowledge into related literature about the impacts of traffic oscillation to traffic flow characteristics.

4.2. Revised car following models with a time gap function

We firstly review some classical car following models.

1) Intelligent driver model

The Intelligent Driver Model (IDM) (Treiber et al. 2000) is given by

$$a_n(t) = a_0\left(1 - \left(\frac{v_n(t)}{v_0}\right)^{\delta} - \left(\frac{s_n^*(t)}{s_n(t)}\right)^2\right), \tag{6}$$

where $s_n^*(t) = s_0 + \max\left(0, v_n(t)T_0 + \frac{v_n(t)\times\Delta v_n(t)}{2\sqrt{a_0 b_0}}\right)$ is the desired gap, v_0 is the desired speed, a_0 is the

maximum acceleration, b_0 is the comfortable deceleration, s_0 is the safety spacing, $\Delta v_n(t) = v_n(t) - v_{n-1}(t)$ is the speed difference between vehicle n and $n-1$, and T_0 is the constant time gap. δ is the exponent, set as 4 in general.

2) Optimal velocity model

The optimal velocity model (OVM) (Bando 1995) is given by

$$a_n(t) = \frac{v_{opt}\big(s_n(t)\big) - v_n(t)}{\tau}, \tag{7}$$

where $v_{opt}\big(s_n(t)\big) = \max\left[0, \min\left(v_0, \frac{s_n(t)-s_0}{T_0}\right)\right]$ defines the "optimal velocity", and τ is the adaptation time.

3) Gipps' model

The Gipps' model (Gipps 1981) is given by

$$v_n(t+\Delta t) = \min\big[v_n(t) + a_0\Delta t, v_0, v_{safe}\big(s_n(t), v_{n-1}(t)\big)\big], \tag{8}$$

where

$$v_{safe}\big(s_n(t), v_{n-1}(t)\big) = -b_0\Delta t + \sqrt{b_0^2\Delta t^2 + v_{n-1}^2(t) + 2b_0(s_n(t) - s_0)}$$

defines the "safe speed", and the simulation update time step Δt is equal to the time gap T_0.

As we known, the time gap is a constant parameter in the above three classical car following models. From the empirical analysis in Section 4.1, however, there exist relationships between the average time gap and other features. Thus, we revise the above classical car following models with Equation (5~~(5)~~). That is to say, the time gap T_0 will be replaced by a time gap function for each vehicle.

4.3. Calibration and validation

The least square error method is applied for parameter calibration, which calculates the mean square error of speed (MSE^v) with the following formulation,

$$MSE^v = \frac{1}{N}\sum_{n=1}^{N}\frac{1}{I_n}\sum_{i=1}^{I_n}\left(v_{ni}^{observed} - v_{ni}^{predicted}\right)^2, \tag{9}$$

where $v_{ni}^{observed}$ is the observed speed of vehicle n at data point i, and $v_{ni}^{predicted}$ is the predicted speed of vehicle n at data point i. Here, the trajectories of the preceding vehicles and the following vehicles' initial states (e.g., locations and speeds) are input data, and the following vehicles' trajectories are output data. And the first 70% data is set as training set and the remaining 30% data is set as validation set.

Table 6 Parameter Bounds and Calibration Results.

	Parameter	Lower bound	Upper bound	Classical model	Revised model
IDM	$a_0\ (m/s^2)$	0.5	3	0.6389	0.6389
	$b_0\ (m/s^2)$	0.5	3	2.2130	0.9167
	$v_0\ (m/s\ )$	10	30	20	26.6667
	$s_0\ (m)$	1	5	1.2222	1.6667
	$T_0\ (s)$	1	5	1.6667	
OVM	$\tau\ (s)$	0.5	1	0.9722	0.9907
	$s_0\ (m)$	1	5	1.0741	1.0741
	$v_0\ (m/s\ )$	10	30	17.037	16.7901
	$T_0\ (s)$	1	5	2.4074	
Gipps'	$a_0\ (m/s^2)$	0.5	3	0.9167	1.1944
	$b_0\ (m/s^2)$	0.5	3	0.5463	0.6389
	$v_0\ (m/s\ )$	10	30	17.7778	17.7778
	$s_0\ (m)$	1	5	1.2222	4.3333
	$\Delta t\ (s)$	1	5	3	

Table 6~~Table 6~~ shows the calibrated parameters of the above classical and revised models. All the parameters are calibrated in a reasonable level. Table 7~~Table 7~~ presents the comparison results between the classical and revised models. We find that all revised models yield better performance than classical models in validation. R-IDM gives a better performance than IDM with 28% improvement. R-OVM gives a better performance than OVM with 40% improvement. And R-Gipps' gives a better performance than Gipps' with 18% improvement.

Table 7 Comparison of fitting results on classical and revised models with the oscillation experiment dataset.

	MSE^v (training)	MSE^v (validation)	IMPROVEMENT
IDM	0.2374	0.2891	
R-IDM	0.2446	0.2089	28% (in validation)
OVM	0.3464	0.4621	
R-OVM	0.2817	0.2791	40% (in validation)
Gipps'	0.2720	0.2759	
R-Gipps'	0.2694	0.2250	18% (in validation)

Figure 12~~Figure 12~~ plots oscillation trajectory examples (the 2nd vehicle in experiment 1) of evolution of speed of the following vehicle with the above classical and revised car following models. The black-dotted curve represents the observed data. The blue dashed curve represents the predicted data of classical models. The red solid curve represents the predicted data of revised models. Figure 12~~Figure 12~~ (a), (b) and (c) plot the results of IDM, OVM and Gipps' model, respectively. We find that the speed trajectory of these three revised models are closer to the observed data compared with the classic models without revision. Thus, with the proposed time gap function, we can replace the constant time gap in classical car following models to yield an improvement in prediction accuracy with the oscillation experiment dataset.

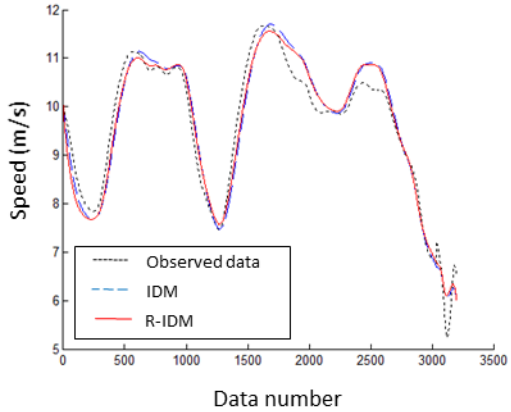

(a)

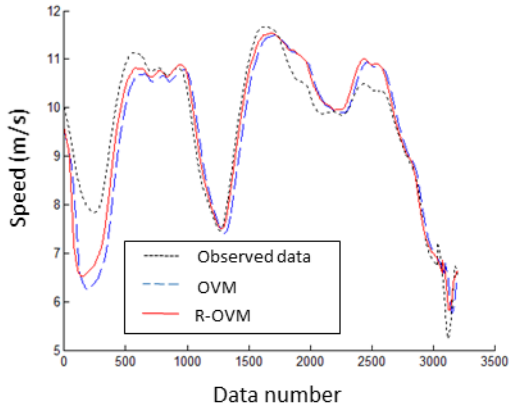

(b)

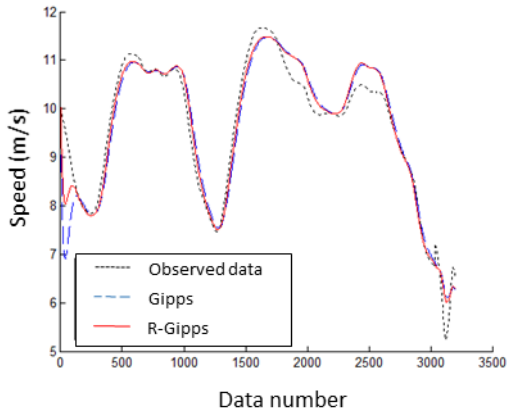

(c)

Figure 12 Oscillation trajectory examples of evolution of speed of the following vehicle with classical and revised models: (a) IDM; (b) OVM; (c) Gipps' model.

Further, we validate the classical and revised models with the stationary trajectory data that was also collected by our field experiments. 7 stationary field experiments were conducted with varying average speed from 10 km/h to 70 km/h with an increment of 10 km/h. The leading vehicle was asked to cruise with the average speed in each stationary field experiment. Table 8~~Table 8~~ shows the validation results on classical and revised models with the stationary experiment dataset. Due to more stable speed in the stationary experiments, the MSEs with the stationary experiment dataset are smaller than those with the oscillation experiment dataset. Compared with the classical models, the revised models still have better performance (with improvement from 29.9% to 63.7%) in the stationary experiment dataset. Further, Figure 13~~Figure 13~~ plots stationary trajectory examples (the 2nd vehicle in experiment 1) of evolution of speed of the following vehicle with the above classical and revised car following models. The example experiment is set with an average speed of 20 km/h. We find that the speed trajectory of these three revised models are closer to the observed data compared with the classic models without revision. Therefore, we can say that the revised models also perform excellent in prediction accuracy with the stationary experiment dataset.

Table 8 Comparison of validation results on classical and revised models with the stationary experiment dataset.

	MSE^v (validation)	IMPROVEMENT
IDM	0.0204	
R-IDM	0.0143	29.9%
OVM	0.0309	
R-OVM	0.0175	43.4%
Gipps'	0.0402	
R-Gipps'	0.0146	63.7%

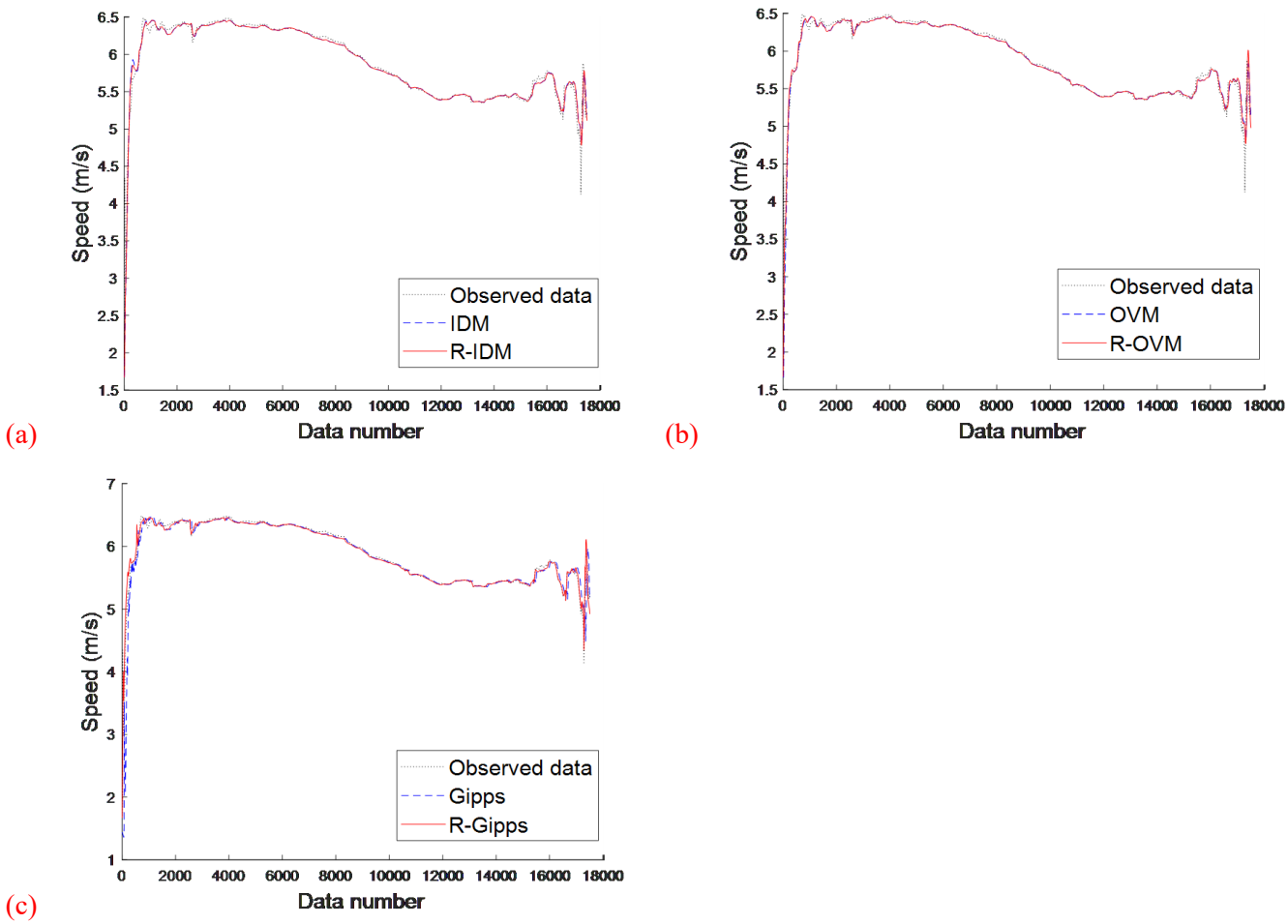

Figure 13 Stationary trajectory examples of evolution of speed of the following vehicle with classical and revised models: (a) IDM; (b) OVM; (c) Gipps' model.

5. CONCLUSION

This paper reports the implementation of a set of field experiments and analyzes the results for the insights into oscillation propagation and associated car-following models. 12 vehicles with high-resolution GPS devices were used to conduct the field tests to investigate the propagation of traffic oscillation. With pre-setting trajectory profiles of the leading vehicle, several traffic oscillation features are specified to investigate the mechanisms of traffic oscillation.

In data processing, oscillation features are measured by a time-domain method. Then, the FT based frequency-domain method is used to verify the effectiveness of the features measured by the time-domain method. The results show that the time-domain method yield comparable measurements with the frequency domain method when the data length is sufficient. Nonetheless, the time-domain method is more robust than the frequency-domain method when the number of oscillation cycles is small. Further, the measurements from the time-domain method have more data points and thus are used in statistical analyses investigating the relationships of traffic oscillation features.

After linear regression analysis, the empirical analysis results shed the following insights not revealed in classic traffic flow models. For example, we find that the average time gap is negatively correlated with the speed standard deviation of the preceding vehicle and the initial speed of the following vehicle, and it is also positively correlated with the average speed of the preceding vehicle and the initial spacing to the preceding vehicle.

According to the above empirical analysis, revised car following models are proposed to capture the relationships between time gap and other traffic features. From the computer simulation results, we find that the revised models with time gap as a function yield better performance in fitting field data compared to the classic car following models with a fixed time gap.

This work provides new empirical data and traffic modeling perspectives and thus can be extended in several directions. We plan to 1) integrate our field data with other data sets, e.g., NGSIM and Jiang's data to reproduce the evolution of speed standard deviation considering different platoon sizes; 2) conduct a set of experiments with higher speeds on freeway to study the impact of high speed on traffic oscillation; and 3) apply the field data with machine learning methods to predict the human driving behavior, or control trajectories of autonomous vehicles.

ACKNOWLEDGEMENTS

The USF team's work is supported by NSF Grants CMMI #1558887 and #1932452. We acknowledge Dr. Jianxun Cui and Dr. Shi An from the Harbin Institute of Technology for their significant efforts in collecting data.

REFERENCES

Aboudina A, Ph D, D HAP, et al (2016) Time-dependent congestion pricing system for large networks : Integrating departure time choice , dynamic traffic assignment and regional travel surveys in the Greater Toronto Area. Transp Res Part A 94:411–430. doi: 10.1016/j.tra.2016.10.005

Ahn S, Cassidy MJ (2007) Freeway traffic oscillations and vehicle lane-change maneuvers. In: Transportation and Traffic Theory 2007. pp 691–710

Arshi AN, Alhajyaseen WKM, Nakamura H, Zhang X (2018) A comparative study on the operational performance of four-leg intersections by control type. Transp Res Part A 118:52–67. doi: 10.1016/j.tra.2018.08.039

Bando M et al. (1995) Dynamical_model_traffic_congestion_and_numerical_simulation.pdf. Phys Rev E 51:1035

Chandler RE, Herman R, Montroll EW (1958) Traffic Dynamics: Studies in Car Following. Oper Res 6:165–184. doi: 10.1287/opre.6.2.165

Chen D, Ahn S, Laval J, Zheng Z (2014) On the periodicity of traffic oscillations and capacity drop: The role of driver characteristics. Transp Res Part B Methodol 59:117–136. doi: 10.1016/j.trb.2013.11.005

Chen D, Laval JA, Ahn S, Zheng Z (2012) Microscopic traffic hysteresis in traffic oscillations: A behavioral perspective. Transp Res Part B Methodol 46:1440–1453. doi: 10.1016/j.trb.2012.07.002

Coifman B, Li L (2017) A critical evaluation of the Next Generation Simulation (NGSIM) vehicle trajectory dataset. 105:362–377. doi: 10.1016/j.trb.2017.09.018

Fernandez R, Yousaf MH, Ellis TJ, et al (2017) Traffic Flow Analysis What is Traffic Flow Analysis ? 131–162

Gipps PG (1981) A behavioural car-following model for computer simulation. Transp Res Part B 15:105–111. doi: 10.1016/0191-2615(81)90037-0

He Z, Zheng L, Guan W (2015) A simple nonparametric car-following model driven by field data. Transp Res Part B Methodol 80:185–201. doi: 10.1016/j.trb.2015.07.010

Herman R, Montroll EW, Potts RB, Rothery RW (1959) Traffic Dynamics: Analysis of Stability in Car Following. Oper Res 7:86–106. doi: 10.1287/opre.7.1.86

Jiang R, Hu M Bin, Zhang HM, et al (2014) Traffic experiment reveals the nature of car-following. PLoS One 9:1–9. doi: 10.1371/journal.pone.0094351

Jiang R, Hu M Bin, Zhang HM, et al (2015) On some experimental features of car-following behavior and how to model them. Transp Res Part B Methodol 80:338–354. doi: 10.1016/j.trb.2015.08.003

Kesting A, Treiber M (2008) How Reaction Time , Update Time , and Adaptation Time Influence the Stability of Traffic Flow. 23:125–137

Knoop V, Hoogendoorn S, van Zuylen H (2008) Capacity Reduction at Incidents: Empirical Data Collected from a Helicopter. Transp Res Rec J Transp Res Board 2071:19–25. doi: 10.3141/2071-03

Laval J, Cassidy M, Daganzo C (2007) Impacts of lane changes at merge bottlenecks: a theory and strategies to maximize capacity. In: Traffic and Granular Flow'05. Springer, pp 577–586

Laval JA (2011) Hysteresis in traffic flow revisited: An improved measurement method. Transp Res Part B Methodol 45:385–391. doi: 10.1016/j.trb.2010.07.006

Laval JA, Leclercq L (2010) A mechanism to describe the formation and propagation of stop-and-go waves in congested freeway traffic. Philos Trans R Soc A Math Phys Eng Sci 368:4519–4541. doi: 10.1098/rsta.2010.0138

Laval JA, Toth CS, Zhou Y (2014) A parsimonious model for the formation of oscillations in car-following models. Transp Res Part B Methodol 70:228–238. doi: 10.1016/j.trb.2014.09.004

Li X, Cui J, An S, Parsafard M (2014) Stop-and-go traffic analysis: Theoretical properties, environmental impacts and oscillation mitigation. Transp Res Part B Methodol 70:319–339. doi: 10.1016/j.trb.2014.09.014

Li X, Ouyang Y (2011) Characterization of traffic oscillation propagation under nonlinear car-following laws. Transp Res Part B 45:1346–1361. doi: 10.1016/j.trb.2011.05.010

Li X, Peng F, Ouyang Y (2010) Measurement and estimation of traffic oscillation properties. Transp Res Part B Methodol 44:1–14. doi: 10.1016/j.trb.2009.05.003

Li X, Wang X, Ouyang Y (2012) Prediction and field validation of traffic oscillation propagation under nonlinear car-following laws. Transp Res Part B Methodol 46:409–423. doi: 10.1016/j.trb.2011.11.003

Li X, Wang Y, Tian J, Jiang R (2018) Stability analysis of stochastic linear car-following models. Transp Sci

Newell GF (1961) Nonlinear Effects in the Dynamics of Car Following. Oper Res 9:209–229. doi: 10.1007/BF00194910

Oh S, Yeo H (2015) Impact of stop-and-go waves and lane changes on discharge rate in recovery flow. Transp Res Part B Methodol 77:88–102. doi: 10.1016/j.trb.2015.03.017

Papageorgiou M (1998) Some remarks on macroscopic traffic flow modelling. 32:323–329

Rakha H, Crowther B (2003) Comparison and calibration of FRESIM and INTEGRATION steady-state car-following behavior. Transp Res Part A 37:1–27

Rhoades C, Wang X, Ouyang Y (2016) Calibration of nonlinear car-following laws for traffic oscillation prediction. Transp Res Part C Emerg Technol 69:328–342. doi: 10.1016/j.trc.2016.05.018

Saifuzzaman M, Zheng Z, Haque MM, Washington S (2017) Understanding the mechanism of traffic hysteresis and traffic oscillations through the change in task difficulty level. Transp Res Part B Methodol 105:523–538. doi: 10.1016/j.trb.2017.09.023

Saxena N, Rashidi TH, Dixit V V, Waller ST (2019) Modelling the route choice behaviour under stop-&-go traffic for different car driver segments. Transp Res Part A 119:62–72. doi: 10.1016/j.tra.2018.11.004

Sun L (2014) Spectral and time-frequency analyses of freeway traffic flow. Transp Res Part A 821–857. doi: 10.1002/atr

Tian J, Jiang R, Jia B, et al (2016a) Empirical analysis and simulation of the concave growth pattern of traffic oscillations. Transp Res Part B Methodol 93:338–354. doi: 10.1016/j.trb.2016.08.001

Tian J, Li G, Treiber M, et al (2016b) Cellular automaton model simulating spatiotemporal patterns, phase transitions and concave growth pattern of oscillations in traffic flow. Transp Res Part B Methodol 93:560–575. doi: 10.1016/j.trb.2016.08.008

Treiber M, Hennecke A, Helbing D (2000) Congested Traffic States in Empirical Observations and Microscopic Simulations. Phys Rev E 62:1805–1824

Treiber M, Kesting A (2012) Validation of traffic flow models with respect to the spatiotemporal evolution of congested traffic patterns. Transp Res Part C Emerg Technol 21:31–41. doi: 10.1016/j.trc.2011.09.002

Treiber M, Kesting A (2017) The Intelligent Driver Model with Stochasticity -New Insights into Traffic Flow Oscillations. Transp Res Procedia 23:174–187. doi: 10.1016/j.trpro.2017.05.011

Yeo H, Skabardonis A (2009) Understanding Stop-and-go Traffic in View of Asymmetric Traffic Theory. Transportation and Traffic Theory 2009: Golden Jubilee. In: Transportation and Traffic Theory 2009: Golden Jubilee. Springer, pp 99–115

Zhang J, Qu X, Wang S (2018) Reproducible generation of experimental data sample for calibrating traffic flow fundamental diagram. Transp Res Part A 111:41–52. doi: 10.1016/j.tra.2018.03.006

Zheng Z, Ahn S, Chen D, Laval J (2011a) Freeway traffic oscillations: Microscopic analysis of formations and propagations using Wavelet Transform. Transp Res Part B Methodol 45 `:1378–1388. doi: 10.1016/j.trb.2011.05.012

Zheng Z, Ahn S, Chen D, Laval J (2011b) Applications of wavelet transform for analysis of freeway traffic: Bottlenecks, transient traffic, and traffic oscillations. Transp Res Part B Methodol 45:372–384. doi: 10.1016/j.trb.2010.08.002

Zheng Z, Ahn S, Monsere CM (2010) Impact of traffic oscillations on freeway crash occurrences. Accid Anal Prev 42:626–636. doi: 10.1016/j.aap.2009.10.009

Zhou M, Qu X, Li X (2017) A recurrent neural network based microscopic car following model to predict traffic oscillation. Transp Res Part C Emerg Technol 84:245–264. doi: 10.1016/j.trc.2017.08.027

Zielke B, Bertini R, Treiber M (2008) Empirical Measurement of Freeway Oscillation Characteristics: An International Comparison. Transp Res Rec J Transp Res Board 2088:57–67. doi: 10.3141/2088-07

APPENDIX A. KEY NOTATION TABLE

Notation	Definition
t	Index of time $t \in \{0, \Delta t, 2\,\Delta t, \dots, T\}$, where T is the maximum time and Δt is a sampling time interval.
k	Index of pre-set cycles $k \in \{1,2, \dots, K\}$, where K is the maximum pre-set cycle.
n	Index of vehicle $n \in \mathbf{N} \coloneqq \{1,2, \dots, N\}$, where $\mathbf{N}$ is the set of vehicles and N is the maximum number of vehicles.
p	Index of time period $p \in \mathbf{P} = \{1,2, \dots, P\}$, where P is the maximum period number.
$x_n(t)$	Location of vehicle $n \in \mathbf{N}$ at time $t \in \mathbf{T}$.
$v_n(t)$	Speed of vehicle $n \in \mathbf{N}$ at time $t \in \mathbf{T}$.
$a_n(t)$	Acceleration of vehicle $n \in \mathbf{N}$ at time $t \in \mathbf{T}$.
tp_{nk}	Cycle length of vehicle $n \in \mathbf{N}$ in traffic oscillation pre-set cycle $k \in \mathbf{K}$.
vmn_{np}	Average speed of vehicle $n \in \mathbf{N}$ in period $p \in \mathbf{P}$.
vsd_{np}	Speed standard deviation of vehicle $n \in \mathbf{N}$ in period $p \in \mathbf{P}$.
tg_{np}	Time gap of vehicle $n \in \mathbf{N}$ in period $p \in \mathbf{P}$.
vin_{np}	Initial speed of vehicle $n \in \mathbf{N}$ in period $p \in \mathbf{P}$.
sin_{np}	Initial spacing of vehicle $n \in \mathbf{N}$ in period $p \in \mathbf{P}$.
$tp.p$	Time period length set of the preceding vehicle.
$tp.f$	Time period length set of the following vehicle.
$vmn.p$	Average speed set of the preceding vehicle.
$vmn.f$	Average speed set of the following vehicle.
$vsd.p$	Speed standard deviation set of the preceding vehicle.
$vsd.f$	Speed standard deviation set of the following vehicle.
tg	Time gap set to the preceding vehicle.
sin	Initial spacing set to the preceding vehicle.
$vin.f$	Initial speed set of the following vehicle.